ETEXT

Optically Pumped Interband Cascade Laser with Graphene Contact

L. J. Olafsen*, K. A. Stephens, and D. R. Sugijanto
Department of Electrical and Computer Engineering, Baylor University
One Bear Place #97356, Waco, TX 76798

Received: 29 July 2021; **Accepted:** 4 August 2021; **Published:** 6 Aug 2021

Citation: L. J. Olafsen*, K. A. Stephens, and D. R. Sugijanto, Optically Pumped Interband Cascade Laser with Graphene Contact (2021): 72-79

Abstract

Lasers comprised of antimonide-based semiconductor materials may be wave function engineered to emit efficiently in the 3–6 μm wavelength range, an atmospheric transmission window that is eye safe and in which chemical sensitivities are 100–10,000 times better than at shorter wavelengths. In particular, the interband cascade laser employs repeated stages to yield multiple photons per injected electron, as compared with a single photon per injected electron in conventional quantum well lasers. However, even with the significant advances achieved utilizing wave function engineering in these semiconductor heterostructures, declining efficiency with increasing current (droop) at high temperatures limits the power output of these lasers. Optical pumping has been used to demonstrate lasing in interband cascade lasers, with the goal of applying this excitation technique to isolate efficiency limiting mechanisms and subsequently improve future laser designs. Integration of graphene layers with high electrical, optical, and thermal conductivity on semiconductor surfaces is presented, with the long-term goal of applying these transparent contact layers to further enhance efficiency. In this work, the spectral characteristics of an ICL with a monolayer graphene top contact evidence a narrower range of emission wavelengths at a given temperature as pump wavelength is varied, as well as systematically increasing differential emission wavelength with temperature as pump wavelength is increased from 1800 nm to 1950 nm.

Keywords: Semiconductor lasers, interband cascade lasers, optical pumping, quantum well lasers, graphene, mid-infrared, spectroscopy

Introduction:

Interband cascade lasers (ICLs) were initially proposed by Yang in 1994 [1] and first demonstrated experimentally in 1997 [2], reaching near-room-temperature operation (286 K) in 1998 [3]. In ICLs, photons are generated at successive steps through interband electron-hole recombination, and carriers are recycled and transport to the next stage via interband tunneling and engineered electron and hole injector layers. The opposite concavity of the conduction and valence bands increases lifetimes and reduces the phonon scattering that accompanies

intersubband transitions in quantum cascade lasers [4]. Above-room-temperature continuous wave operation was achieved in ICLs in 2008 [5]. Rebalancing electron and hole densities, complemented by increased doping in the electron injectors [6] reduced threshold intensities and increased efficiencies, but ICLs have continued to suffer efficiency droop above room temperature [7,8].

To explore the contribution of carrier non-pinning above threshold to the efficiency droop, Ikyo *et al*. measured spontaneous emission as a function of temperature and of pressure [7]. Because stimulated emission intensity is much larger than spontaneous emission intensity in the plane of the laser cavity, a window was milled in the substrate of the ICL to collect spontaneous emission off-axis. An alternate approach to collect spontaneous emission is to employ a transparent contact on the surface that facilitates uniform bias and current injection while transmitting the mid-infrared (mid-IR) spontaneous emission. While indium-tin-oxide is a well-known material for transparent contacts, transmission cuts off in the near-IR, reducing suitability for collecting mid-IR spontaneous emission. The potential of graphene as a suitable transparent contact is pursued here, with the long-term goal of collecting spontaneous emission under bias as well as for carrier excitation by optical pumping [9–12]. Tunable optical excitation has been used to demonstrate resonant excitation, with corresponding threshold minimization and slope efficiency maximization in type-II W [13] antimonide-based semiconductor lasers [9,10]. Optical pumping also has been used to achieve lasing in unprocessed ICL wafers [14].

Perfect graphene is a two-dimensional hexagonal lattice of carbon atoms, first observed as a single atomic layer in 1962 [15] and the subject of the Nobel Prize in Physics in 2010 [16,17]. While graphene is considered in one perspective to be highly absorbing, given that each layer is only one-atom thick, the fact that it can be deposited as a single or a few layers translates to transparencies of >90%, as each monolayer absorbs $\pi\alpha \approx 2.3\%$ [18], where α is the fine structure constant. The transmission is flat and broadband [18,19], with little-to-no degradation extending into the infrared. Seminal work revealing the optical conductivity (transmission) [18] and thermal conductivity [20] has been performed on graphene films suspended in vacuum. These characteristics, coupled with high electrical conductivity, make graphene a promising candidate for a transparent contact. This contact may be Schottky or ohmic depending upon the relative work functions of the graphene and the underlying semiconductor capping layer along with fabrication or annealing conditions.

Integration of graphene contacts is presented here as a tool to help identify the physical mechanisms leading to efficiency droop, with the long-term goal of circumventing these losses through modifications and improvements to future device designs, including epitaxy and fabrication. This work is a first step in that process, presenting spectral output data for optically pumped ICL samples, both with and without a monolayer graphene top contact. Results are presented for optical pump wavelengths varying from 1800 nm to 1950 nm and temperatures varying from 80 K to 200 K.

Materials and Methods:

The ICLs were grown by molecular beam epitaxy at Naval Research Laboratory on *n*-GaSb substrates. An InAs/AlSb superlattice bottom optical cladding layer and a 400–600-nm-thick *n*-GaSb bottom separate confinement layer (SCL) were grown below 10 active stages, where gain was produced by type-II InAs/GaInSb/InAs/AlSb "W" quantum wells [13]. A top SCL, top optical cladding layer, and *n*+-InAs top contact layer were grown above the active stages. To "rebalance" the electron and hole carrier densities [6], four InAs quantum wells in each electron injector of each active stage were heavily *n* doped.

Monolayer graphene was grown on copper substrates by chemical vapor deposition (CVD) at Rice University [21]. The graphene was transferred to the ICL wafer. That wafer then was cleaved to a cavity length of 2 mm and attached using silver paint to an oxygen free high thermal conductivity (OFHC) copper heat sink below an uncoated sample that was cleaved to a cavity length of 3 mm. The copper heat sink was mounted to the cold finger of an Advanced Research Systems optical cryostat, in which the sample temperature was controlled from 80 K to 300 K.

Optical pumping [10] was achieved using the idler output of a Nd:YAG-pumped optical parametric oscillator (Spectra-Physics primo-Scan). The pump pulse duration was ~10 ns, with a repetition rate of 10 Hz. Optical pump intensity was controlled using a half wave retarder with a broadband polarizing cube beam splitter, maintaining a constant incident polarization. Wavelengths for the optical pumping ranged from 1800 nm to 1950 nm. These pump wavelengths were chosen based upon previous optical pumping experiments on antimonide-based mid-IR semiconductor lasers, balancing maximum absorption of the pump beam and transmission of the pump beam through the substrate (for epi-side-down mounting) while minimizing photon decrement [9–12]. Pump stripe widths of ~1 mm were achieved using cylindrical lenses.

Spectral measurements were taken using a Horiba iHR550 Mid-Focal Length Imaging spectrometer with a grating with 300 grooves per nm that was blazed at 4000 nm. Signal was detected with a DSS-IS020L Indium Antimonide Solid State Detector powered by a DSS-15VP Low Noise Power Amplifier. The detector was connected via BNC cable to a Stanford Research Systems (SRS) Lock-in Model 810 triggered by the Q-switch from the Nd:YAG laser, and spectra were acquired using Horiba's LabSpec6 software.

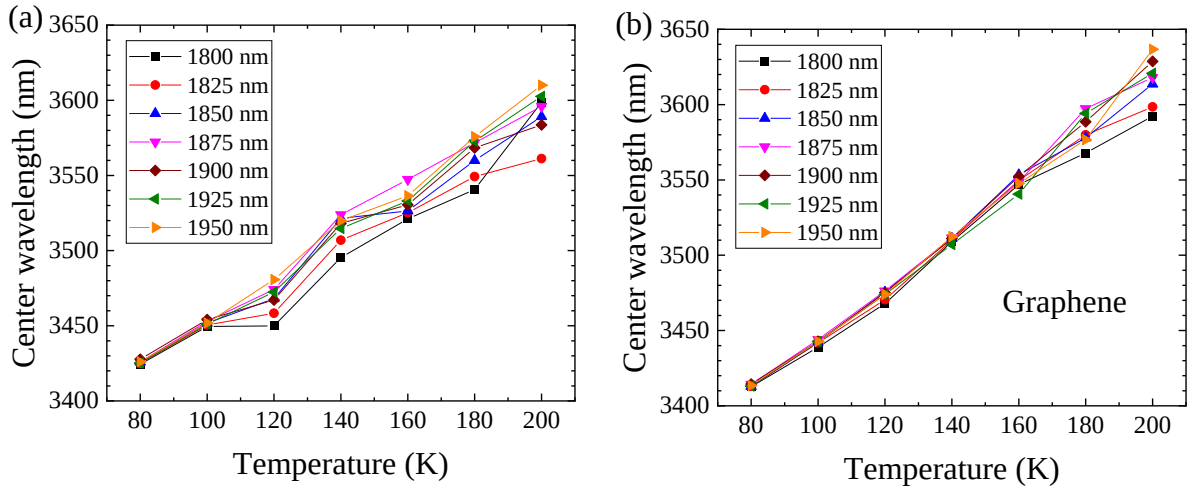

Figure 1: Center wavelength (in nm) vs. heat sink temperature (K), obtained from Gaussian fits to spectral data. The data shown in (a) is for a 3-mm-long ICL with no top contact and the data in (b) is for a 2-mm-long ICL with a monolayer graphene layer atop the InAs cap.

Results

Emission spectra were collected for both samples, optically pumped at wavelengths from 1800 nm to 1950 nm, at temperatures in the 80–200 K range. As the pump stripe widths were relatively wide, these broad-area spectra not surprisingly were multimodal. The center wavelengths of the Gaussian fits to the emission spectra as a function of temperature are shown in Figure 1 for the ICLs (a) without and (b) with a graphene monolayer. In Figure 2, the center wavelength data is shown as a function of pump wavelength rather than as a function of temperature as shown in Figure 1. As in Figure 1, the plots of Figure 2 are (a) without and (b) with a graphene monolayer. Data is shown for pump wavelengths in 25 nm steps and temperature in 20 K steps.

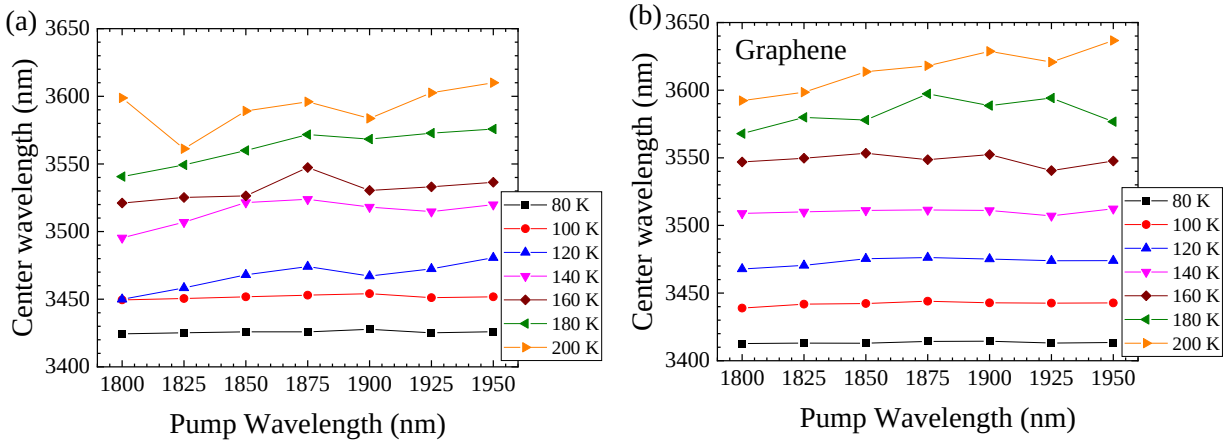

Figure 2: Center wavelength (nm) vs. pump wavelength (nm), obtained from Gaussian fits to spectral data. The data shown in (a) is for a 3-mm-long ICL with no top contact, and the data in (b) is for a 2-mm-long ICL with a monolayer graphene layer atop the InAs cap.

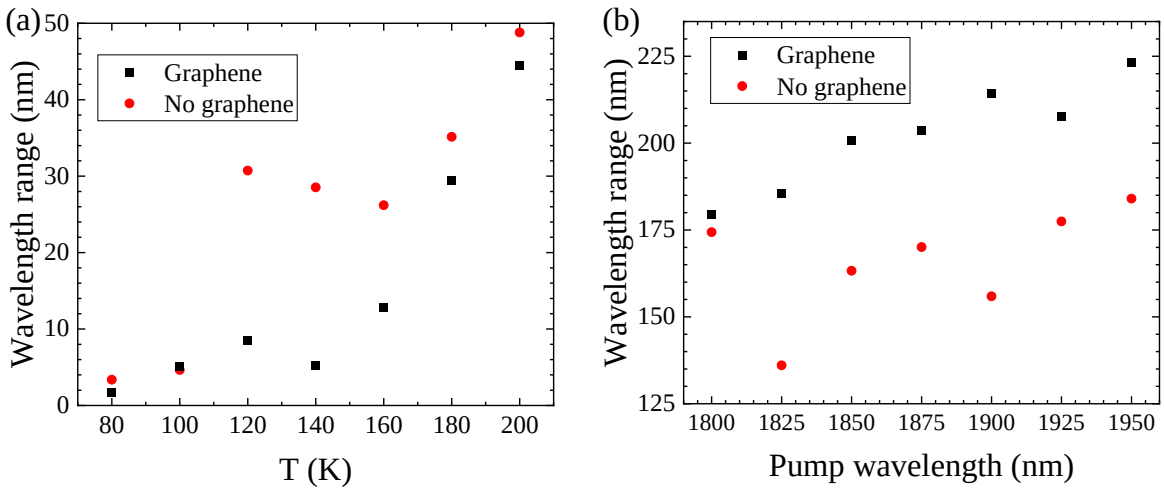

Figure 3: The range of center wavelengths as a function of (a) temperature and (b) pump wavelength for ICL samples with (black squares) and without (red circles) monolayer graphene top contact layers.

The wavelength range, calculated as the difference between the maximum and minimum wavelengths, is shown in Figure 3 as a function of (a) temperature for the full range of pump wavelengths (corresponding to Figure 1) and of (b) pump wavelength for the full range of temperatures (corresponding to Figure 2). These three figures provide different visualizations of the variation of center wavelength as a function of temperature and of pump wavelength. For the ICL without graphene, the variation with pump wavelength is relatively small (<5 nm) at 80 K and 100 K, but that variation is observed to be larger (25–50 nm) at temperatures greater than or equal to 120 K. The range of center wavelengths for graphene is less than 2 nm at 80 K and less than 10 nm up through 140 K. At 160 K the range increases to approximately 13 nm, and the larger range of wavelengths only is observed at 180 K and 200 K.

Figure 3(b) illustrates the range of center wavelengths as a function of pump wavelength. As this range represents the variation in wavelength over a 120 K temperature variation, the larger wavelength range values of 125–225 nm, corresponding to expected temperature-dependent red shifts of 1–2 nm/K. While the uncoated ICL sample demonstrates a range that is not clearly systematic, the range for the graphene-coated sample is increasing as a function of pump wavelength. This systematic behavior for the graphene-contact sample is further illustrated in Figure 4(a), which plots the slope of a linear fit to the center wavelength vs. temperature data shown in Figure 1. This ordinate is the differential of the center emission wavelength as a function of temperature. While the sample without graphene shows behavior that is generally increasing, but with some larger variation from 1.2 to 1.5 nm/K, the data for the graphene-coated sample is more systematic, increasing approximately linearly from 80 K to 160 K, and possibly flattening out at the higher temperatures.

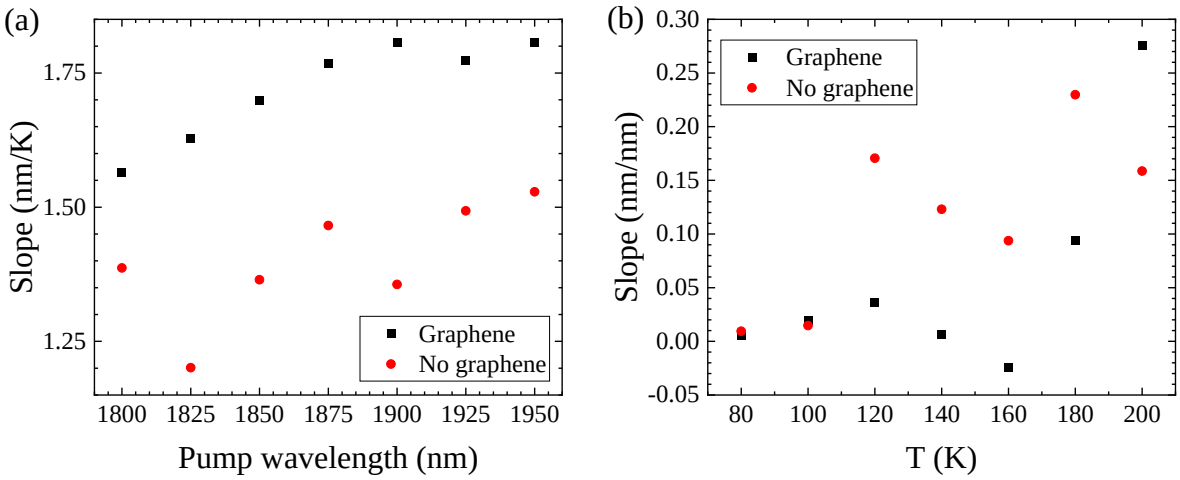

Figure 4: (a) The slope of the center wavelength vs. temperature data (from Figure 1) as a function of pump wavelength. (b) The slope of the center wavelength vs. pump wavelength data (from Figure 2) as a function of temperature.

A general increase of differential center output wavelength as a function of pump wavelength is shown as a function of temperature in Figure 4(b). The behavior mimics (but does not duplicate) the temperature trends in Figure 3(a), another indication of stability introduced by the graphene monolayer up through temperatures of 140 K to 160 K.

Relative to the uncoated, optically pumped ICL sample, the ICL with a graphene monolayer indicates more stable spectral emission (narrower wavelength range) as a function of temperature, as well as demonstrating a systematic increase of output wavelength per unit temperature as a function of pump wavelength. One potential explanation of the emission spectra trends for the graphene-coated ICL sample is that the high thermal conductivity of graphene could be dissipating heating of the epitaxial structure that results from the photon decrement associated with the optical pumping. Alternately, the nature of the graphene-semiconductor contact, expected to be Schottky due to the difference in graphene and InAs work functions, may result in bending of bands that affects internal bias and transport of carriers photogenerated by optical pumping. Further investigation of this behavior as a function of pump wavelength as well as temperature may help to quantify internal bias correlated with generated photovoltage and ultimately to investigate alignment and band filling that could help determine the source of carrier non-pinning postulated to be causing the efficiency droop at high temperatures in ICLs.

Conclusion

An interband cascade laser with a monolayer graphene top contact demonstrated lasing, and its output characteristics were compared with an uncoated cavity of the same device. Stability (narrower range) of center emission wavelengths for the graphene-coated samples is observed, as well as a more systematic temperature dependence of the wavelength shift than for the uncoated sample. Future work will include optical pumping at narrower beam width, repeating measurements on these ICLs, and comparisons with and without graphene contacts in other devices (other MBE growths). Because the measurements were performed on different pieces of

the same wafer, it is possible that the overall wavelength shifts were due to pumping a different section of the wafer, but the relative and systematic shifts are of great interest for further investigation.

Acknowledgement

The authors acknowledge Dr. Jerry R. Meyer and co-workers at the Naval Research Laboratory for providing the ICL wafer materials. The authors also acknowledge Dr. James Tour and Dr. Zhiwei Peng at Rice University for graphene CVD growth and transfer. This work was supported by the National Science Foundation, Award Number 1256113.

References

[1] R. Q. Yang, "Infrared laser based on intersubband transitions in quantum wells," *Superlattices and Microstructures* **77**, 77–83 (1995).

[2] C. H. Lin, R. Q. Yang, D. Zhang, S. J. Murry, S. S. Pei, A. A. Allerman, and S. R. Kurtz, "Type-II interband quantum cascade laser at 3.8 μm," *Electronics Letters* **33**, 598–599 (1997).

[3] L. J. Olafsen, E. H. Aifer, I. Vurgaftman, W. W. Bewley, C. L. Felix, J. R. Meyer, D. Zhang, C. H. Lin, and S. S. Pei, "Near-room-temperature mid-infrared interband cascade laser," *Applied Physics Letters* **72**, 2370–2372 (1998).

[4] J. Faist, F. Capasso, D. Sivco, C. Sirtori, A. L. Hutchinson, and A. Cho, "Quantum cascade laser," *Science* **264**, 553–556 (1994).

[5] M. Kim, C. L. Canedy, W. W. Bewley, C. S. Kim, J. R. Lindle, J. Abell, I. Vurgaftman, and J. R. Meyer, "Interband cascade laser emitting at λ = 3.75 μm in continuous wave above room temperature," *Applied Physics Letters* **92**, 191110 (2008).

[6] I. Vurgaftman, W. W. Bewley, C. L. Canedy, C. S. Kim, M. Kim, *et al*., "Rebalancing of internally generated carriers for mid-infrared interband cascade lasers," *Nature Communications* **2**, 585 (2011).

[7] B. A. Ikyo, I. P. Marko, A. R. Adams, S. J. Sweeney, C. L. Canedy, I. Vurgaftman, C. S. Kim, M. Kim, W. W. Bewley, and J. R. Meyer, "Temperature dependence of 4.1 μm mid-infrared type II 'W' interband cascade lasers," *Applied Physics Letters* **99**, 021102 (2011).

[8] C. D. Merritt, W. W. Bewley, C. S. Kim, C. L. Canedy, I. Vurgaftman, J. R. Meyer, and M. Kim, "Gain and loss as a function of current density and temperature in interband cascade lasers," *Applied Optics* **54**, F1–F7 (2015).

[9] L. J. Olafsen and T. C. McAlpine, "Transparency pump intensity and differential gain in resonantly pumped W optical pumping injection cavity lasers," *Journal of Applied Physics* **108**, 053106 (2010).

[10] L. J. Olafsen, "Tunable Optical Pumping Technique for the Development of Mid-Infrared Semiconductor Lasers," Chapter 11, New Developments in Photon and Materials Research, J. I. Jang, Ed. New York: Nova Science Publishers, 2013.

[11] C. L. Felix, W. W. Bewley, I. Vurgaftman, L. J. Olafsen, D. W. Stokes, *et al*., "High-efficiency midinfrared 'W' laser with optical pumping injection cavity," *Applied Physics Letters* **75**, 2876–2878 (1999).

[12] T. C. McAlpine, K. R. Greene, M. R. Santilli, L. J. Olafsen, W. W. Bewley, *et al*., "Resonantly pumped optical pumping injection cavity lasers," *Journal of Applied Physics* **96**, 4751–4754 (2004).

[13] J. R. Meyer, C. A. Hoffman, F. J. Bartoli, and L. R. Ram-Mohan, "Type-II quantum-well lasers for the mid-wavelength infrared," *Applied Physics Letters* **67**, 757–759 (1995).

[14] L. J. Olafsen and N. Rumman, "Optically Pumped Mid-Infrared Interband Cascade Lasers," *2020 IEEE Texas Symposium on Wireless and Microwave Circuits and Systems (WMCS)*, Waco, TX, USA, 2020, pp. 1-4.

[15] H. P. Boehm, A. Clauss, G. O. Fischer and U. Hofmann, "Thinnest Carbon Films," *Zeitschrift für Naturforschung* **17**, 150–153 (1962).

[16] K. S. Novoselov, "Graphene: Materials in the Flatland (Nobel Lecture)," *Angewandte Chemie* **123**, 7123–7141 (2011); *Angewandte Chemie International Edition* **50**, 6986–7002 (2011).

[17] A. K. Geim, "Random Walk to Graphene (Nobel Lecture)," *Angewandte Chemie* **123**, 7100–7122 (2011); *Angewandte Chemie International Edition* **50**, 6966–6985 (2011).

[18] R. R. Nair, P. Blake, A. N. Grigorenko, K. S. Novoselov, T. J. Booth, T. Stauber, N. M. R. Peres, and A. K. Geim, "Fine Structure Constant Defines Visual Transparency of Graphene," *Science* **320**, 1308 (2008).

[19] F. Bonaccorso, Z. Sun, T. Hasan, and A. C. Ferrari, "Graphene photonics and optoelectronics," *Nature Photonics* **4**, 611–622 (2010).

[20] A. A. Balandin, S. Ghosh, W. Bao, I. Calizo, D. Teweldebrhan, F. Miao, and C. N. Lau, "Superior thermal conductivity of single-layer graphene," *Nano Letters* **8**, 902–907 (2008).

[21] Z. Yan, Z. W. Peng, and J. M. Tour, "Chemical Vapor Deposition of Graphene Single Crystals," *Accounts of Chemical Research* **47**, 1327 (2014). https://doi.org/10.1021/ar4003043